Force Fields for Metallic Clusters and Nanoparticles

NICOLE LEGENSKI,[1] CHENGGANG ZHOU,[2] QINGFAN ZHANG,[2] BO HAN,[2] JINPING WU,[2] LIANG CHEN,[3] HANSONG CHENG,[2,4] ROBERT C. FORREY[1]

[1]*Department of Physics, Penn State University, Berks Campus, Reading, Pennsylvania 19610-6009*
[2]*Sustainable Energy Laboratory, China University of Geosciences, Wuhan, 430074, China*
[3]*Ningbo Institute of Materials Technology and Engineering, Ningbo, Zhejiang 315201, China*
[4]*Department of Chemistry, National University of Singapore, 3 Science Drive, Singapore 117543*

Received 1 October 2010; Revised 10 December 2010; Accepted 18 December 2010
DOI 10.1002/jcc.21753
Published online 1 March 2011 in Wiley Online Library (wileyonlinelibrary.com).

Abstract: Atomic force fields for simulating copper, silver, and gold clusters and nanoparticles are developed. Potential energy functions are obtained for both monatomic and binary metallic systems using an embedded atom method. Many cluster configurations of varying size and shape are used to constrain the parametrization for each system. Binding energies for these training clusters were computed using density functional theory (DFT) with the Perdew-Wang exchange-correlation functional in the generalized gradients approximation. Extensive testing shows that the many-body potentials are able to reproduce the DFT energies for most of the structures that were included in the training set. The force fields were used to calculate surface energies, buk structures, and thermodynamic properties. The results are in good agreement with the DFT values and consistent with the available experimental data.

 J Comput Chem 32: 1711–1720, 2011

Key words: potential energy function; force field; clusters; nanoparticles

Introduction

In a recent publication,[1] an atomic force field (FF) for simulating copper clusters and nanoparticles was described. A fast and reliable FF obtained as gradients of a potential energy function (PEF) allows molecular dynamics simulations to be carried out for systems where first principle electronic structure-based simulations would be too computationally intensive to be of practical use. The FF and PEF may also be used to investigate the evolution of structure and properties of clusters and nanoparticles. Detailed understanding of the growth of metal nanostructures would allow particle sizes and shapes to be controlled during synthesis for a variety of applications including heterogeneous catalysis. The catalytic properties of gold nanoparticles, for example, exhibit a well-known size dependence.[2,3] Size-dependent thermodynamic variables are generally difficult to measure. Understanding the mechanisms of growth and evaporation often requires the use of simulations based on an analytic and transferable PEF. Parametrization of the PEF using bulk data may lead to significant errors for the energies of small clusters and nanoparticles, as has been shown for the case of aluminum.[4] Since the formation process may involve the coalescence of nanostructures and small clusters, it is desirable to develop analytic and transferable PEFs that are capable of describing clusters and nanoparticles of all sizes and shapes.

The PEF that was developed for copper[1] was able to reproduce *ab initio* binding energies for equilibrium and nonequilibrium structures for cluster sizes ranging from only a few atoms to large nanoparticles that approach bulk structure. The parametrization of the copper PEF was constrained by more than 2000 cluster configurations of varying size and shape. The binding energies of these training clusters were computed using density functional theory (DFT) under the generalized gradients approximation (GGA) with the Perdew-Wang exchange-correlation functional (PW91) as implemented in DMol[3] package. A similar approach has been adopted in this work for gold and silver clusters and nanoparticles. The training sets include more than 12,000 and 7,000 cluster configurations for gold and silver, respectively.

Binary metallic alloys may be used to form metallic glasses that lack the long-range order of normal crystalline metals. Large clusters within a metallic glass are often formed by the interconnection of smaller clusters.[5,6] Therefore, an accurate account of both small and large cluster behavior may be important for understanding the formation mechanisms of these noncrystalline binary metallic systems.

The development of a binary FF based on the PEF described in[1] poses a difficulty, which is anticipated in this work. Namely,

Correspondence to: H. Cheng; e-mail: chmch@nus.edu.sg (or) R. C. Forrey; e-mail: rcf6@psu.edu

Contract/grant sponsor: The National Science Foundation; contract/grant number: PHY-0854838

the form of the PEF for small clusters was fundamentally different from that which was used for large clusters. This procedure allowed detailed modeling of small clusters through use of a bond-order function, which contained information on the local environment. For larger clusters, the bond-order function was replaced by an embedded atom (EA) method,[7] which had sufficient accuracy and was computationally more efficient. While this procedure works well for monatomic systems, it is problematic for binary systems. Therefore, we investigate in this work the use of a single form for the PEF, which would allow extensions to binary metallic systems to be more readily developed. Due to a desire to maintain computational efficiency for large clusters and nanoparticles, we excluded bond-order functions that contain a summation over a third atomic site index and considered only PEFs, which are based on an EA method. An appropriate balance between accuracy, transferability, and computational efficiency is achieved by training the FF using a weighting scheme which emphasizes near-equilibrium structures and large cluster sizes.

For both monatomic and binary systems, we use the PEF to compute the average error per atom for a large range of cluster sizes and shapes. The binary PEFs are designed to reduce to the monatomic PEFs in the appropriate limits. The use of combination rules, which interpolate between monatomic parameters to obtain binary parameters without any additional training is investigated. An improvement scheme is developed, which uses training sets comprised of binary clusters of many sizes, shapes, and alloy ratios. These additional training sets were computed using DFT as described above and included more than 5,000 configurations for each of the binary systems (Cu + Ag, Cu + Au, and Ag + Au).

Form of the PEF

The quantum Sutton-Chen (QSC) model is one of the most reliable of the EA methods and is the basis of the PEF used in this work. The QSC model[8] is capable of providing accurate values for surface energies, vacancy energies, stacking-fault energies, and cohesive energies in the bulk limit.[9,10] The general form of the PEF is given by

$$E = \sum_i \left[\frac{1}{2} \sum_{j \neq i} D_{ij} V(r_{ij}) - c_{ii} D_{ii} \rho_i^{1/2} \right] \tag{1}$$

$$V(r_{ij}) = \left(\frac{\alpha_{ij}}{r_{ij}} \right)^{p_{ij}} \tag{2}$$

$$\rho_i = \sum_{j \neq i} \left(\frac{\alpha_{ij}}{r_{ij}} \right)^{q_{ij}} \tag{3}$$

where the square root of the density-like quantity ρ_i provides an embedding function that accounts for many-body effects. Parametrization of this PEF using bulk data generally leads to poor performance for small clusters and nanoparticles.[1,4] The same is true, however, when atomic pair potentials are used to construct the PEF even when a bond-order coefficient is included to account for many-body effects. The variation of metallic bonds for different cluster sizes and shapes is too large to be adequately described with a fixed set of parameters. To overcome this difficulty, parameters that depend on the local environment were used in a Morse type PEF, and the agreement with *ab initio* DFT calculations was greatly improved.[1] This approach also employed the use of a bond-order function,[11,12] which contains a summation over a third atomic site index. This additional summation greatly reduces the computational efficiency of the PEF as the number of atoms in the cluster increases. The QSC form (1) provides a more compact representation of the PEF compared to those which use a bond-order function. If the QSC parameters are allowed to also depend on the local environment, particularly for small clusters and nanoparticles, then the reliability of the QSC-type of PEF should improve.

Parametrization

To extend the reliability of a QSC-type PEF to sub-bulk systems, it is convenient to introduce an effective coordination number

$$M_i = \sum_{j=1}^{N} l_C(r_{ij}) - 1 \tag{4}$$

for atom i. The local cutoff function $l_C(r)$ allows the number of neighboring atoms to be counted with a weighting that depends on distance. Although not required, $l_C(r)$ is assumed in this work to be the same as a smooth cutoff function $f_C(r)$, which multiplies the pair potentials in eqs. (2) and (3) to reduce the computational effort by eliminating large distance contributions. It is defined to be zero when $r > r_{\max}$ and one when $r < r_{\min}$ with a smooth connection

$$f_C(r) = \frac{1}{2} \left[1 + \cos \left(\frac{\pi (r - r_{\min})}{r_{\max} - r_{\min}} \right) \right] \tag{5}$$

in between. Similar to,[1] we generalize the potential parameters in eqs. (1)–(3) to allow a dependence on the local environment. In this case, however, this dependence is considerably simpler as only one atomic site index is required. Also, the dependence on a "global" coordination number, which introduced small discontinuities in the FF for break-up channels[1] is removed in this work. The parameters are defined by

$$D(M_i) = D_0 + (D_1 - D_0) \cdot \mathrm{Min}(12, M_i)/12 \tag{6}$$

$$c(M_i) = c_0 + (c_1 - c_0) \cdot \mathrm{Min}(12, M_i)/12 \tag{7}$$

$$\alpha(M_i) = \alpha_0 + (\alpha_1 - \alpha_0) \cdot \mathrm{Min}(12, M_i)/12 \tag{8}$$

$$p(M_i) = p_0 + (p_1 - p_0) \cdot \mathrm{Min}(12, M_i)/12 \tag{9}$$

$$q(M_i) = q_0 + (q_1 - q_0) \cdot \mathrm{Min}(12, M_i)/12 \tag{10}$$

These parameters provide a linear dependence on M_i before reaching a constant value when the effective coordination reaches the bulk value of 12. For this reason, we refer to FF's that use this parameterization as FF1. For comparison, we use FF0 to refer to the usual QSC-type of FF, which contain parameters without the M_i-dependence shown in (6)–(10). For binary metallic systems, the parameters are defined by

Table 1. FF_0 Parameters for Copper, Silver, and Gold.

	D_0 (eV)	c_0	α_0 (Å)	p_0	q_0
Cu	0.97251	1.25718	2.03707	12.51465	2.54495
Ag	0.52735	1.67790	2.47532	12.45291	1.80458
Au	0.65415	1.82580	2.54173	12.31934	3.55212

$$D(M_i, N_i) = D(M_i) + (D_2 - D_0) \cdot \mathrm{Min}(12, N_i)/12 \quad (11)$$

$$c(M_i, N_i) = c(M_i) + (c_2 - c_0) \cdot \mathrm{Min}(12, N_i)/12 \quad (12)$$

$$\alpha(M_i, N_i) = \alpha(M_i) + (\alpha_2 - \alpha_0) \cdot \mathrm{Min}(12, N_i)/12 \quad (13)$$

$$p(M_i, N_i) = p(M_i) + (p_2 - p_0) \cdot \mathrm{Min}(12, N_i)/12 \quad (14)$$

$$q(M_i, N_i) = q(M_i) + (q_2 - q_0) \cdot \mathrm{Min}(12, N_i)/12 \quad (15)$$

where M_i is the number of nearest neighbors of the same type as atom i and N_i is the number of nearest neighbors of a different type as atom i. For both monatomic and binary systems, the parameters in eqs. (1)–(3) are obtained from the combination rules

$$D_{ij} = \sqrt{D(M_i, N_i) \cdot D(M_j, N_j)} \quad (16)$$

$$c_{ij} = \frac{1}{2}[c(M_i, N_i) + c(M_j, N_j)] \quad (17)$$

$$\alpha_{ij} = \frac{1}{2}[\alpha(M_i, N_i) + \alpha(M_j, N_j)] \quad (18)$$

$$p_{ij} = \frac{1}{2}[p(M_i, N_i) + p(M_j, N_j)] \quad (19)$$

$$q_{ij} = \frac{1}{2}[q(M_i, N_i) + q(M_j, N_j)] \quad (20)$$

For FF0, the combination rules are the same as those used previously.[9,10] For a monatomic system, the coordination numbers N_i and N_j are zero and the parameters (16)–(20) reduce to those given in eqs. (6)–(10). The FF0 and FF1 parameters for the three metallic systems are given in Tables 1 and 2. Note that although FF0 is of the same form as the standard QSC-type of FF which are designed to reproduce bulk properties, the parameters given here are very different due to the training sets which include small and intermediate sized clusters. For FF1, the addition of the linear terms in the parametrization requires that the constant parameters (with subscript zero) are recomputed and are generally not the same as for FF0. In all calculations, the values of $r_{\min}$ and $r_{\max}$ were set to 3 and 5 Å, respectively.

Table 2. FF_1 Parameters for Copper, Silver, and Gold.

	i	D_i (eV)	c_i	α_i (Å)	p_i	q_i
Cu	0	0.13961	3.96788	2.68496	11.26408	10.24328
Cu	1	0.82566	1.93253	2.22857	7.96061	3.15717
Ag	0	0.25590	2.70378	2.86178	11.07230	10.42481
Ag	1	1.02952	1.51273	2.46059	8.68235	3.84122
Au	0	0.84105	1.67526	2.54055	12.74993	10.68084
Au	1	1.88295	1.14705	2.43205	9.83923	4.84162
Cu + Ag	2	0.72848	2.02081	2.28822	8.02453	2.48090
Cu + Au	2	0.92499	2.01610	2.38057	7.96796	2.67050
Ag + Cu	2	1.11780	1.57238	2.52451	8.00608	4.34362
Ag + Au	2	1.09787	1.70548	2.73388	8.61485	3.48297
Au + Cu	2	1.96652	1.29905	2.43940	9.35256	7.98669
Au + Ag	2	2.07570	1.42034	2.36455	9.48098	10.61060

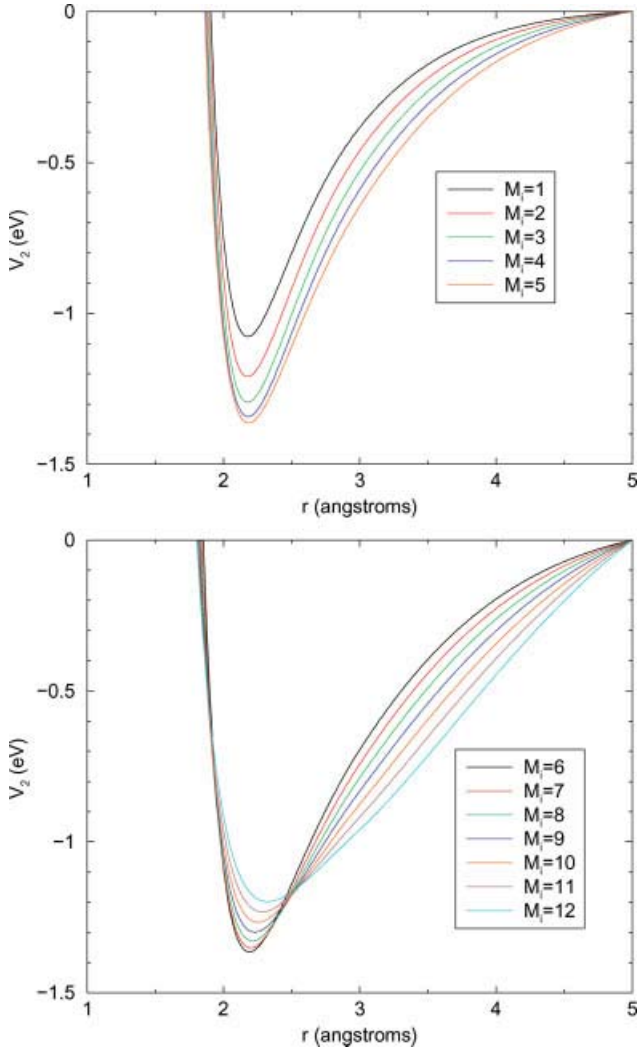

Figure 1. Modifications to the Cu 2-body potential due to increasing the number of nearest neighbors of atom i. Top panel is for $M_i = 1 - 5$ and the bottom panel is for $M_i = 6 - 12$.

Results

The FF was trained using *ab initio* DFT data by computing the function

$$f(N) = \frac{\sum_{\mathrm{m}}^{M_{\mathrm{N}}} w_{\mathrm{m}} \left| E_{\mathrm{m}}^{\mathrm{DFT}} - E_{\mathrm{m}}^{\mathrm{FF}} \right|}{N \sum_{\mathrm{m}}^{M_{\mathrm{N}}} w_{\mathrm{m}}} \quad (21)$$

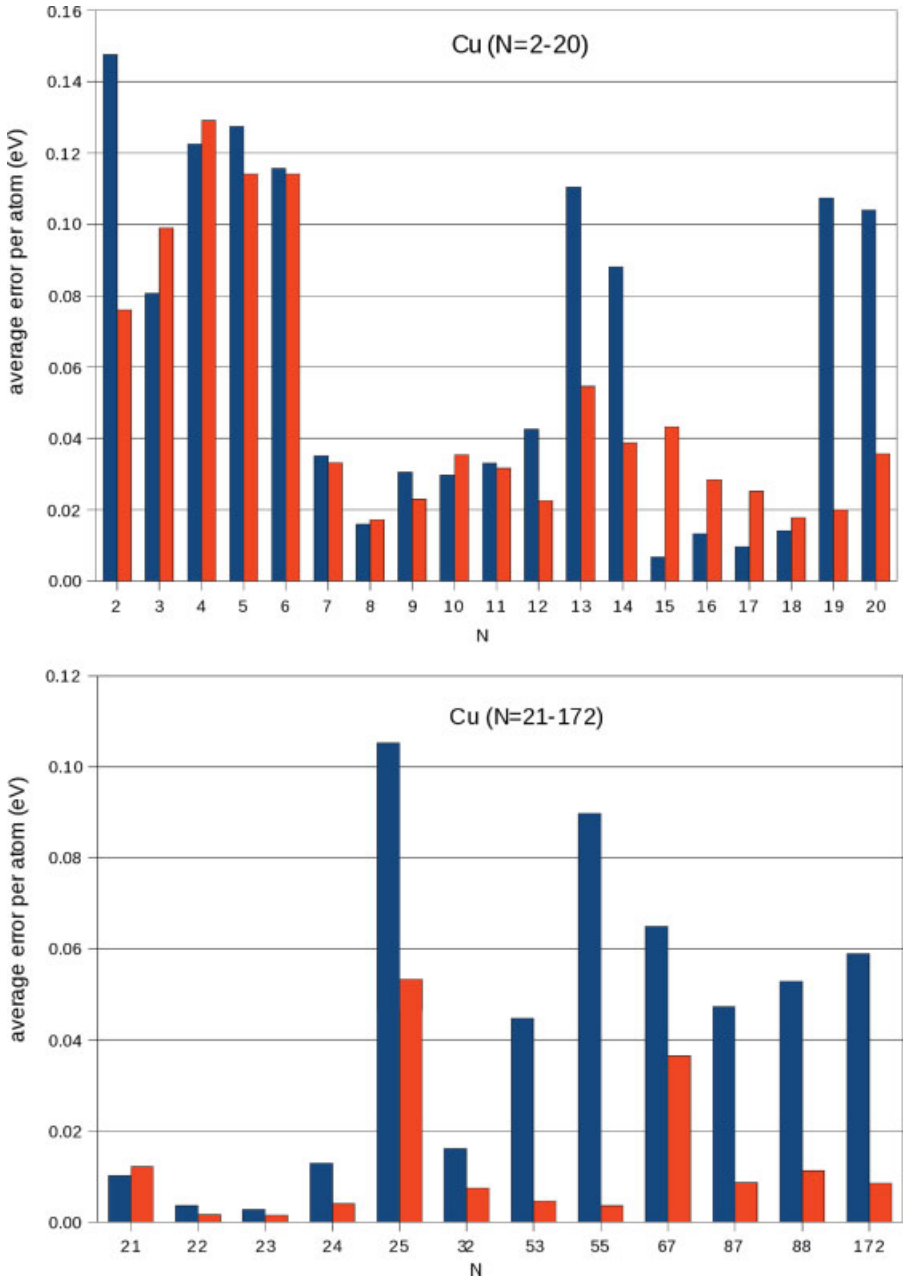

Figure 2. Average error per atom for Cu clusters. Top panel is for $N = 2 - 20$ and the bottom panel is for $N = 21 - 172$. FF0 results are shown in blue and FF1 results in red.

where M_N is the number of cluster configurations of size N, and E_m^{DFT} and E_m^{FF} are the respective DFT and FF energies for the m-th configuration. The weight function was chosen to be the absolute value of the DFT energy per atom. This weighting emphasizes the lowest energy equilibrium structures without significantly neglecting the non-equilibrium structures and metastable isomers. Higher energy structures are also fairly well-described in most cases using this procedure. All cluster sizes are trained simultaneously by minimizing the function

$$g = \frac{\sum_N^{N_{max}} N f(N)}{\sum_N^{N_{max}} N} \tag{22}$$

The size-dependent weighting in (22) helps to ensure an appropriate limit as cluster sizes approach the bulk. After the PEF has been trained to fit the DFT data, the PEF is used to compute energy minima using all structures in the DFT training set as starting points for the optimization. This is a critical step in establishing the reliability of

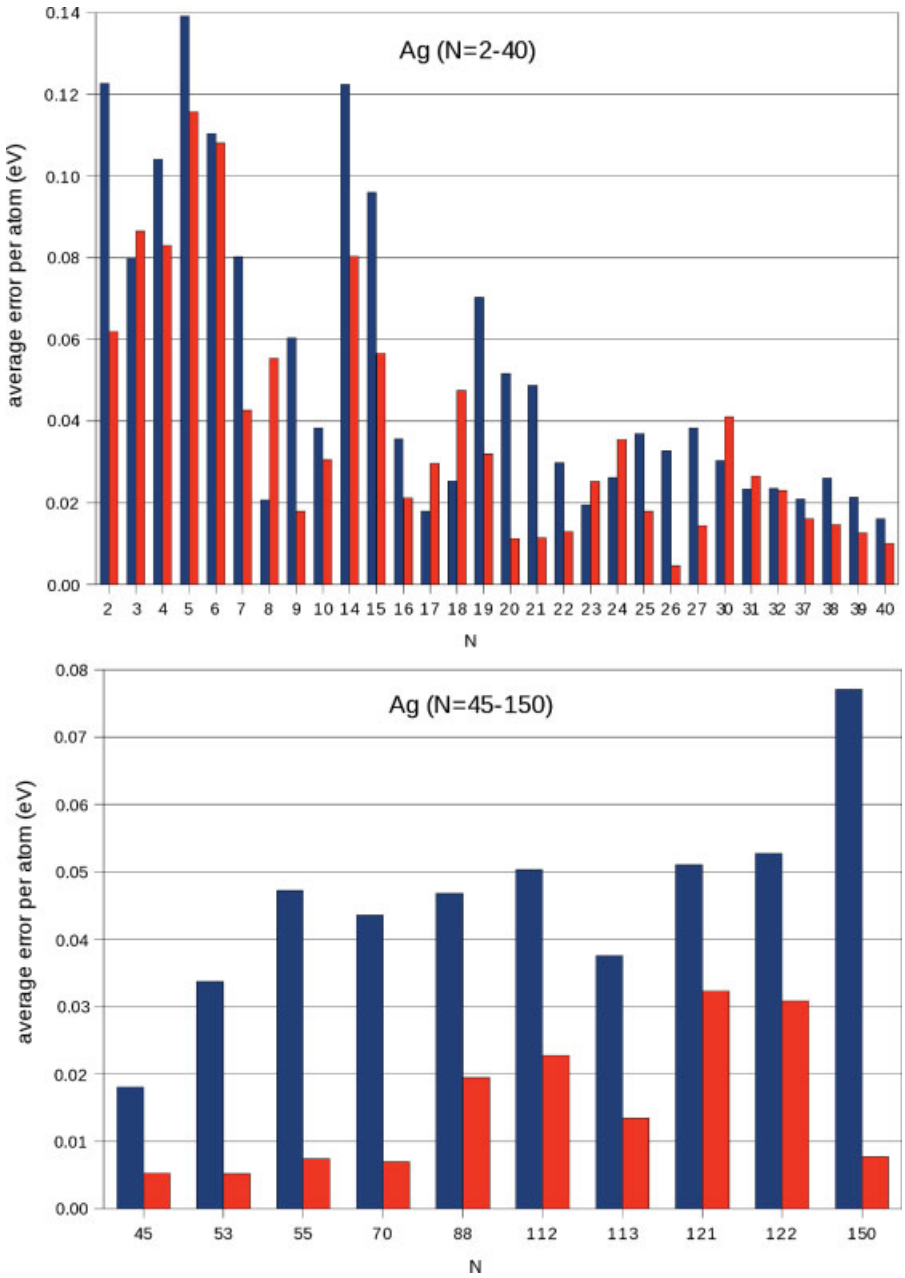

Figure 3. Average error per atom for Ag clusters. Top panel is for $N = 2 - 40$ and the bottom panel is for $N = 45 - 150$. FF0 results are shown in blue and FF1 results in red. [Color figure can be viewed in the online issue, which is available at wileyonlinelibrary.com.]

the FF as it is not uncommon to obtain a PEF which provides a good fit to the DFT data but produces energy minima that are well-below expectations. Typically, this occurs when the DFT training set does not include enough nonequilibrium structures with compressed bonds. In such cases, the DFT training set is updated to include the minimum energy structures obtained by the PEF and a retraining is performed.

The optimized M_i-dependent parameters typically modify the 2-body potential in a pattern such as shown in Figure 1 for Cu. Initially, as the number of nearest neighbors of atom i increases, the 2-body potential becomes progressively deeper while remaining at roughly the same equilibrium position. This is shown in the top panel of Figure 1. As M_i increases further, the potential becomes more shallow and the equilibrium position pushes outward towards the bulk value. This is seen in the bottom panel of Figure 1, which also shows that the long-range part of the potential becomes more attractive.

Figure 2 shows the average error per atom for Cu clusters. FF0 results are shown in blue and FF1 results in red. For small clusters with $N \leq 6$, the results show relatively large errors for both

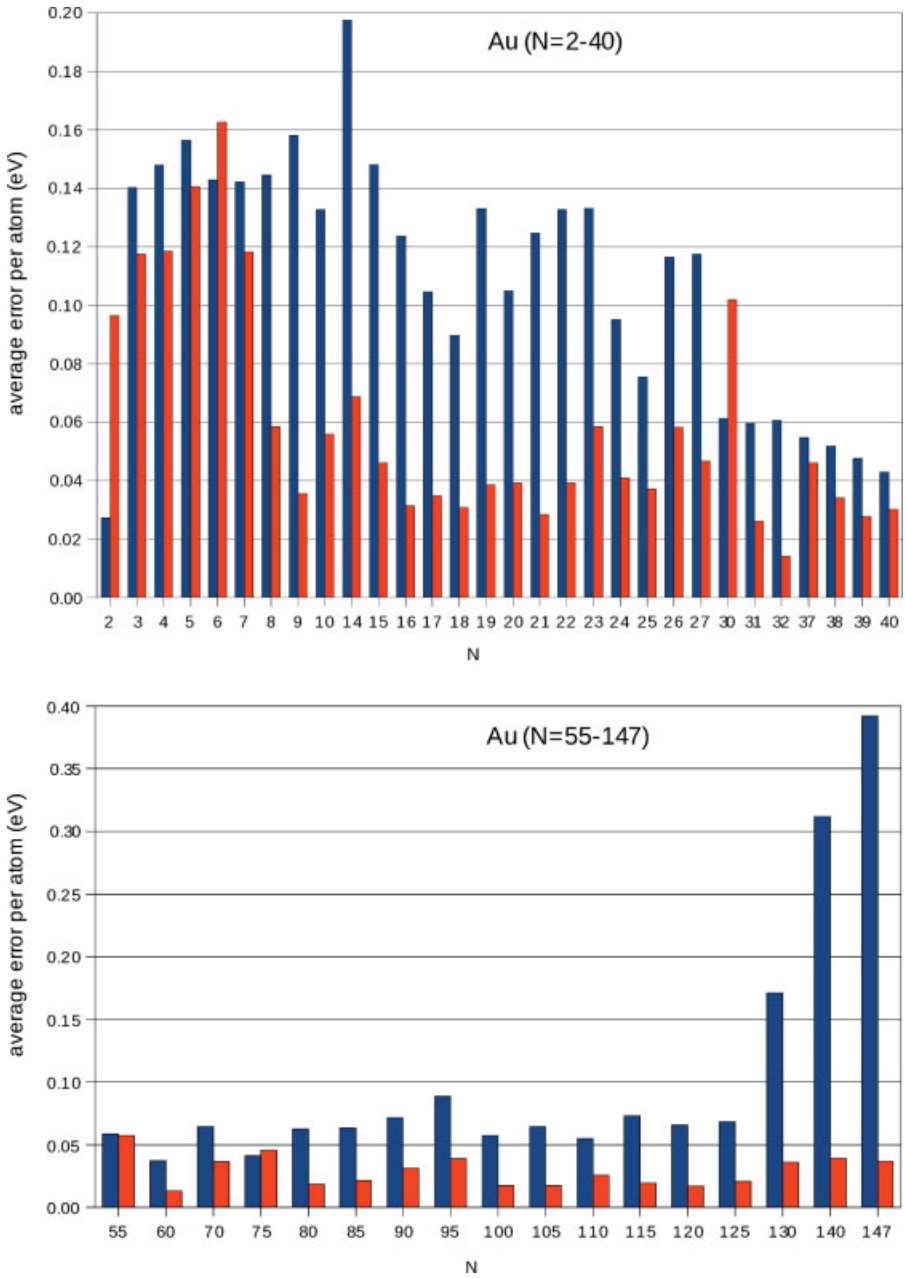

Figure 4. Average error per atom for Au clusters. Top panel is for $N = 2 - 40$ and the bottom panel is for $N = 55 - 147$. FF0 results are shown in blue and FF1 results in red. [Color figure can be viewed in the online issue, which is available at wileyonlinelibrary.com.]

FF0 and FF1. For these cluster sizes, the *ab initio* minimum energy structures are two-dimensional.[13,14] This poses a challenge for PEFs that are based on an embedded atom model due to the preference for close packing in the model, which generally leads to three-dimensional (3D) structures having the lowest energy. For $N \geq 7$, the minimum energy structures are 3D and the average error per atom is substantially improved for both parametrizations. The FF0 results, however, show large errors for some specific cluster sizes (e.g. $N = 13, 14, 19, 20, 25$, and 55), which include a number of icosahedral-type configurations in the training set. The FF1 results are significantly better for these sizes. Clusters with $N > 55$ were not included in the training set to test whether the PEF was capable of extrapolating to larger clusters and nanoparticles. Again, the FF1 results are significantly better than the FF0 results for cluster sizes up to $N = 172$.

Figures 3 and 4 show the average error per atom for Ag and Au clusters, respectively. The trends for Ag clusters are similar to those of the Cu clusters shown in Figure 2. The errors for small $N < 7$ clusters are again large due to the difficulty in describing minimum energy structures that are 2-dimensional. For larger sizes, the FF1

Table 3. Training Set for Cu_mAg_n Clusters.

m/n	1	2	3	4	5	6	7	8	9	11	13	14	16	19	20	22	23	24	27	30	31	36
1	92	246	135	28	45	19	29	191	126									42				
2	254	140	51	83	30	27	28	29												139		55
3	63	71	63	156	33	63	68															
4	64	67	180	33		76																
5	58	34	36	72	44										33				146			
6	23	86	51	43																		
7	25	32	71																		165	
8	45	43																282				
9													32				277					
11												51										
14										59												
16																253						
17								55														
19														100								
25											70											

The number of different cluster configurations is shown for each (m, n) pair included in the training set.

Table 4. Training Set for Au_mAg_n Clusters.

m/n	1	2	3	4	5	6	7	8	9	10	11	12	13	16	17	19	20	22	24	26
1	97	327	89	59	34	41	48	32	51			30						24		
2	117	153	121	19	70	47	57	43				18								
3	45	47	167	16	31	56	71			33				40						
4	40	42	166	87	34	155			86	22						72				
5	32	28	101	119	63			65									86			
6	22	30	157	201			33	19								65				
7	52	29	50			67								80						
8	176	51			100	19					105				96				166	
9	62			75						173										
10			77	23					59											
11		37																		
12	27	22					147													220
13												204				159				
14					119				80		231									
15										168										
16														122						
18	151				24															
19													164							
21		97																		
22			159																	
23									137											
26												107								
28				125																
34				28																

results are substantially better than the FF0 results, particularly for the largest clusters that were considered. As in the case of Cu, the Ag clusters with $N > 55$ were not included in the training set in order to test the extrapolation capability of the PEFs. The FF0 results show that the average error per atom tends to get larger as the cluster size increases, whereas the FF1 errors are acceptable for all sizes up to $N = 150$. In the case of Au clusters, the comparison between the FF0 and FF1 results is even more striking. Due to a slower evolution to minimum energy stuctures which are 3D, we used $N = 2 - 100$ clusters in the Au training set. Figure 4 shows that the FF0 results are acceptable for cluster sizes at the high end of the training set but are poor for $N < 30$ and $N > 125$. The FF1 results show dramatic improvement for nearly all cluster sizes and appear to extrapolate nicely to large-N for each of the three metallic systems.

For binary systems, the $i = 2$ parameters in Table 2 were obtained using the training sets shown in Tables 3–5. The number of different configurations is indicated in the tables for binary clusters Cu_mAg_n, Au_mAg_n, and Au_mCu_n. These configurations include most of the stable and metastable isomers for small cluster sizes as well as some representative near-equilibrium structures for the larger cluster

Table 5. Training Set for Au_mCu_n clusters.

m/n	1	2	3	4	5	6	7	8	9	10	11	12	14	15	16	19	20	22	23	25
1	97	217	81	59	18		35	65	38			16								
2	221	109	117	62		173	67	43			56	18								
3	63	75	75		24	64	40			18					39			177		
4	46	129		97	80	27			47	18						124				
5	41		35	35	27			320									170			
6		53	70	43			58	25												
7	25	173	59			133									76					
8	23	41			120	172					96									
9	33			497						107					129				96	
10			94	21					37											
11		48						157				96	165							
12	18	21																		
13																121				77
14					84				118		133									
17						27		145						120						
18	80																			
20					458							125								
22	29														85					
23		74																		
24								127												
27											136									
28				48																
32						137														

sizes. Figure 5 shows the average error per atom for binary metallic alloys comprised of Cu, Ag, and Au atoms. For Cu + Ag clusters, the FF0 results appear to be satisfactory as N increases. This PEF uses the combination rules (16)–(20) with no additional training. Some improvement is seen in the FF1 results which required an additional training step beyond the initial training of the monatomic clusters. A more substantial benefit of this additional training step (i.e., to obtain the $i = 2$ parameters in Table 2) is seen when Au is used as one of the metals. For both of the Au alloys, the average error per atom is unacceptably large for nearly all cluster sizes when FF0 is used. The FF1 results are considerably better with an average error per atom typically less than 0.05 eV for $N > 6$. We found that the unsatisfactory performance of FF0 is due to an interesting synergy that occurs for binary alloys containing gold atoms. Binding energies for the alloy clusters are typically greater for a particular structure than for the same stucture comprised of either of the constituent metals. Combination rules, which use only the monatomic parameters, cannot account for this synergy. The increased flexibility provided by the linear terms in eqs. (11)–(15) allows an adequate account of the synergy and a significantly improved description of the binary clusters.

The FF parameters developed here were fitted only to the data obtained from DFT calculations on small metal clusters and no bulk data were used. To test the applicability of the force field to condensed phase systems, we imposed a periodic boundary condition to the chosen bulk metals and the selected surfaces (Cu, Ag, Au). All the atomic coordinates and lattice parameters were first fully optimized using a conjugate gradient algorithm and the calculated structural parameters are all in good agreement with the DFT calculated geometries. For bulk metals, we carried out lattice dynamics simulations to derive cohesive energies and thermodynamic quantities upon full structural equilibration. The results are shown in Table 6, where the corresponding DFT and experimental values are also listed. Reasonable agreement between the FF-derived data and the DFT and experimental values is achieved. We further calculated the surface energies of Cu(111), Ag(111), and Au(111) surfaces. Comparison between the FF results and the corresponding DFT and experimental values is shown in Table 7. The FF surface energies are in reasonable agreement with the DFT values but somewhat smaller than the experimental data.

Conclusions

In this work, we have developed an embedded atom PEF that leads to the efficient computation of an atomic FF. The form of the PEF is similar to the QSC-type[8] but with parameters that are explicitly dependent on the local environment. The parameters increase linearly with coordination number for sub-bulk systems and become constant when the bulk coordination is reached. This approach retains the well-established effectiveness of the QSC-type FF for bulk systems[9,10] while allowing significant improvements to be made for clusters and nanoparticles.

The form of the PEF allows a straight-forward extension to binary metallic systems. Through use of the combination rules (16)–(20), the parameters of the PEF may be trained in two steps using *ab initio* data. The first training step obtains the necessary parameters for any desired monatomic system. The second step allows the parameters to be modified for binary systems while preserving

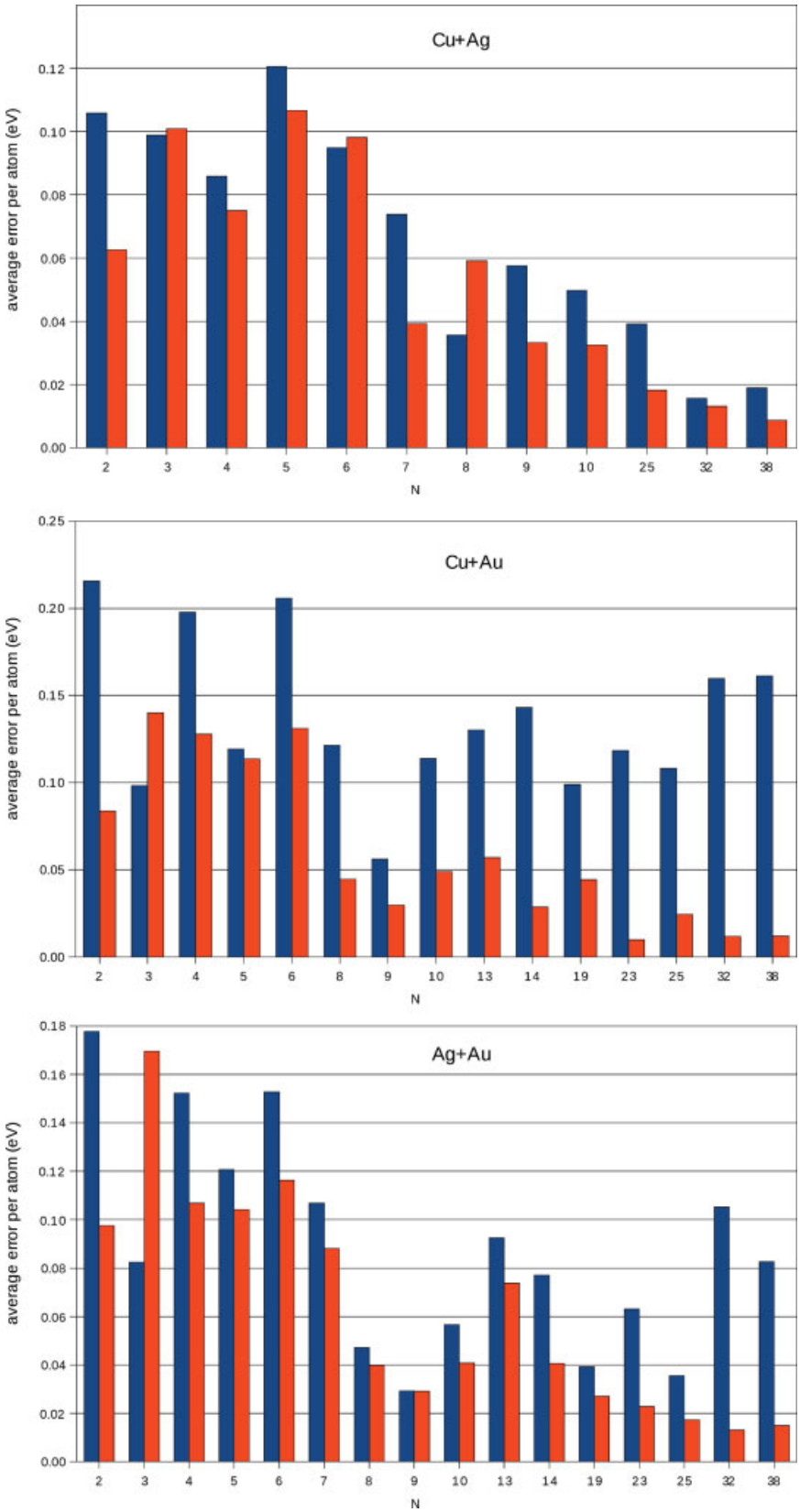

Figure 5. Average error per atom for binary clusters. Top panel is for Cu + Ag, the middle panel is for Cu + Au, and the bottom panel is for Ag + Au. FF0 results are shown in blue and FF1 results in red. [Color figure can be viewed in the online issue, which is available at wileyonlinelibrary.com.]

Table 6. Comparison of the Calculated Cohesive Energies, Entropies, and Heat Capacities at Room Temperature and the Experimental Values.

	Cohesive energy (eV)			S^0 (J/K · mol)			Cp^0 (J/K · mol)		
	Exp.	DFT	FF	Exp.	DFT	FF	Exp.	DFT	FF
Cu	3.49	3.41	3.30	33.15	33.71	31.96	24.44	23.65	23.3
Ag	2.95	2.42	2.59	42.55	43.05	39.98	25.35	24.32	24.46
Au	3.81	2.90	3.05	47.40	48.70	42.99	25.42	24.52	23.77

Table 7. Comparison of the Calculated Surface Energies (eV/atom).

	FF	DFT	Exp.
Cu(111)	0.53	0.53	0.64
Ag(111)	0.45	0.54	0.56
Au(111)	0.50	0.60	0.67

the monatomic parametrizations in the appropriate limits. Additional steps for ternery and larger systems could be easily introduced to obtain further extensions of this procedure. The present results demonstrate that this procedure is capable of producing FFs, which are transferable, computationally efficient, and reliable. The average error is less than 0.05 eV/atom for nearly all cluster sizes. Only in the case of small isolated molecules does the PEF perform poorly. This is due to the difficulty in describing minimum energy structures that are 2D. It is unlikely that such isolated structures would affect the ability of the PEF to describe cluster growth since new additions are known to take place preferentially at sites, which allow multiple neighboring atoms.[14] In cases where a small isolated molecule is part of an entrance or exit channel, the present PEFs would introduce a larger average error ($\sim$0.1 eV/atom) and would require modification.

We tested the performance of the FF for predicting physical properties of bulk metals and surfaces against the DFT and experimental results. It was found that the predicted bulk structures, cohesive energies, and thermodynamic properties are in good agreement with both DFT and experimental results. The FF-calculated surface energies are also in reasonable agreement with the corresponding DFT values, however, both DFT and FF calculations are somewhat smaller than the reported experimental data. Considering the fact that the FF parameters were developed entirely based on DFT calculations on small clusters and no bulk properties were used for the FF parameter fitting, this agreement is encouraging. We believe that the FF parameters may be further improved by accounting for bulk properties using either DFT or experimental data.

References

1. Zhou, C.; Wu, J.; Chen, L.; Wang, Y.; Cheng, H.; Forrey, R. C. Comput Chem 2009, 30, 2255.
2. Hashmi, A. S. K. Chem Rev 2007, 107, 3180.
3. Hashmi, A. S. K.; Frost, T. M.; Bats, J. W. J Am Chem Soc 2000, 122, 11553.
4. (a) Jasper, A. W.; Staszewski, P.; Staszewska, G.; Schultz, N. E.; Truhlar, D. G. J Phys Chem B 2004, 108, 8996; (b) Jasper, A. W.; Schultz, N. E.; Truhlar, D. G. J Phys Chem B 2005, 109, 3915.
5. Yavari, A. R. Nature 2006, 439, 405.
6. Sheng, H. W.; Luo, W. K.; Alamgir, F. M.; Bai, J. M.; Ma, E. Nature 2006, 439, 419.
7. (a) Daw, M. S.; Baskes, M. I. Phys Rev Lett 1983, 50, 1285; (b) Daw, M. S.; Baskes, M. I. Phys Rev B 1984, 29, 6443.
8. Sutton, A. P.; Chen, J. Philos Mag Lett 1990, 61, 139.
9. Qi, Y.; Cagin, T.; Kimura, Y.; Goddard, W. A., III. Phys Rev B 1999, 59, 3527.
10. Lee, H.-J.; Cagin, T.; Johnson, W. L.; Goddard, W. A., III. J Chem Phys 2003, 119, 9858.
11. Tersoff, J. Phys Rev B 1988, 37, 6991.
12. Brenner, D. W. Phys Rev B 1990, 42, 9458.
13. Guvelioglu, G. H.; Ma, P.; He, X.; Forrey, R. C.; Cheng, H. Phys Rev Lett 2005, 94, 026103.
14. Guvelioglu, G. H.; Ma, P.; He, X.; Forrey, R. C.; Cheng, H. Phys Rev B 2006, 73, 155436.